Efficient Soft X-Ray Lasing at 6 to 8 nm with Nickel-like Lanthanide Ions

H. Daido, Y. Kato, K. Murai, S. Ninomiya, R. Kodama, G. Yuan, Y. Oshikane, M. Takagi, and H. Takabe
Institute of Laser Engineering, Osaka University, 2-6 Yamada-oka, Suita, Osaka 565, Japan

F. Koike
Physics Laboratory, School of Medicine, Kitasato University, 1-15-1 Kitasato, Sagamihara, Kanagawa 228, Japan
(Received 3 November 1994)

We report the demonstration of efficient soft x-ray lasing in nickel-like lanthanide elements (Nd, Sm, Gd, Tb, and Dy) covering the spectral range between 6 and 8 nm. A curved slab target was pumped by 1.053-μm-wavelength multiple laser pulses: two or three 100-ps-duration pulses separated by 400 ps. A gain coefficient of 3.1 cm^{-1} and a gain-length product of 7.8 have been achieved at 7.97 nm in the Nd ions with 250 J pumping energy on a 2.5-cm-length target. The result represents close to an order of magnitude reduction in the energy required to pump these soft x-ray lasers.

PACS numbers: 42.55.Vc, 34.50.Fa

Successful results on soft x-ray amplification have been achieved with the electron collisional excitation scheme including neonlike and nickel-like isoelectronic sequences [1–3]. With the neonlike scheme, the required pumping laser intensity increases rapidly as the wavelength becomes shorter towards the water window spectral region (4.4–2.3 nm) [4].

According to the calculation based on the collisional radiative equilibrium model [5], the plasma parameters required for the Ni-like laser media [6] of lanthanide elements with $Z = 60$–66 are almost the same as those for the Ne-like germanium (Ge; $Z = 32$) laser [2], where Z is the atomic number. Europium (Eu; $Z = 63$) [7] and ytterbium (Yb; $Z = 70$) [8] lasers have been successfully demonstrated by pumping with a 1-ns laser pulse of several kJ energy and 0.53 μm wavelength. The gain coefficients of these were ~ 1 cm^{-1}, whereas that of the Ni-like tantalum (Ta; $Z = 73$) laser was 2.3 cm^{-1} pumped with almost the same laser condition in spite of its shorter lasing wavelength [9]. These results imply that further optimization of the pumping parameters such as the wavelength and the pulse width for matching to the desired lasing plasmas could make the Ni-like soft x-ray lasers more efficient.

In this Letter, we describe the demonstration of efficient Ni-like lanthanide soft x-ray lasers with the spectral range between 6 and 8 nm by pumping a curved slab target [10,11] with multiple infrared pulses [12,13] with an energy of $\sim$250 J on a 2.5-cm-length target which is an order of magnitude lower than that for the previous Eu laser experiment [7]. The lasing materials include Nd ($Z = 60$), Sm ($Z = 62$), Gd ($Z = 64$), Tb ($Z = 65$), and Dy ($Z = 66$). A gain coefficient of 3.1 cm^{-1} and a gain-length product of 7.8 have been achieved at 7.97 nm.

A curved slab target [11] is composed of a 200-μm-wide and 1-μm-thick stripe-shaped lasing material of a pure lanthanide element coated on a 0.9-mm-thick glass (SiO_2) plate, which was bent to an angle θ by applying suitable mechanical stress to the glass plate in order to prevent refraction decoupling of the x-ray laser beam from the gain region. The bent angle of 10 mrad for a 2.5-cm-long target, corresponding to a 2.5-m radius of curvature, provided the most intense lasing for the Ni-like Nd soft x-ray laser. This result is very similar to that for the Ne-like Ge laser [13]. The target was irradiated within a few hours after it was taken out from the coating chamber in order to prevent oxidation of the lasing material. A laser beam of 1.053 μm wavelength (one of the twelve Gekko X II laser beams) was focused to a line of 2.8 cm length and $\sim$70 μm average width. The laser pulse was composed of two or three pulses with the individual pulse width of 100 ps separated by 400 ps. The laser energy was $\sim$130 J for each 100 ps pulse corresponding to the average irradiance of 6.9×10^{13} W/cm^2 at the line-focus area. An on-axis spectrometer was composed of a cylindrical mirror and a grazing incidence flat field grating with the average groove number of 1200 lines/mm [14]. The spectra were recorded either with an Ilford Q2 plate for time-integrated and angle-resolved measurement or with an x-ray streak camera for time-resolved measurement at a specific horizontal angle [15]. The temporal resolution of the streak camera was 25 ps.

The absolute wavelengths of the spectrograph were determined by the first, second, and third order diffraction spectra of the lasing lines with an iterative method using the grating equation. The accuracy of this method is within ± 0.04 nm at 8 nm, limited mainly by the resolving power of the spectrometer which is $\lambda/\Delta\lambda \sim 200$ in the present experiment where λ and $\Delta\lambda$ are the center wavelength and the lasing linewidth on a Q2 plate, respectively. Uncertainty in the distance between the grating and the detector causes a systematic error for wavelength determination, which is estimated to be 0.05 nm at 8 nm. The measured wavelengths of the $J = 0$-1 lasing lines are listed in Table I. Also shown in this table are the wavelengths and

 0031-9007/95/75(6)/1074(4)$06.00

TABLE I. Measured and calculated wavelengths (in nm) and the calculated oscillator strengths of the Ni-like $J = 0$-1 lasing lines. Also shown are the radiative decay times from the lower lasing levels to the ground state (in ps). The notation * denotes "unable to measure."

		$_{60}$Nd	$_{62}$Sm	$_{64}$Gd	$_{65}$Tb	$_{66}$Dy
$J = 0$-1 $(\frac{3}{2}, \frac{3}{2})$	Measured wavelength	7.97	7.32	6.92	6.67	6.37
	Calculated wavelength	7.937	7.375	6.866	6.632	6.409
to $(\frac{5}{2}, \frac{3}{2})$	Calculated oscillator strength	0.253	0.228	0.207	0.197	0.188
	Radiative decay time	0.362	0.306	0.260	0.240	0.222
$J = 0$-1 $(\frac{3}{2}, \frac{3}{2})$	Measured wavelength	*	*	6.39	6.11	5.88
	Calculated wavelength	7.448	6.865	6.334	6.090	5.856
to $(\frac{3}{2}, \frac{1}{2})$	Calculated oscillator strength	0.169	0.182	0.193	0.199	0.204
	Radiative decay time	0.988	0.740	0.569	0.503	0.446

the oscillator strengths that we have calculated using an unpublished version (GRASP2 developed by Parpia *et al.* in 1992) of GRASP (general purpose relativistic atomic structure program) [16]. The calculated wavelengths agree with the experimental results within the measurement accuracy and with the former calculation [17].

Figure 1 shows the spectra of the Ni-like Nd, Sm, Gd, and Tb lasers recorded with an x-ray streak camera [18]. In Fig. 1, each spectrum is composed of two $J = 0$-1 lines; a longer wavelength line due to the $3d^9 4d(\frac{3}{2}, \frac{3}{2}) \rightarrow 3d^9 4p(\frac{5}{2}, \frac{3}{2})$ transition and a shorter wavelength line due to the $3d^9 4d(\frac{3}{2}, \frac{3}{2}) \rightarrow 3d^9 4p(\frac{3}{2}, \frac{1}{2})$ transition indicated by the arrows. In our experimental results, the intensity of the longer wavelength $J = 0$-1 line dominates for all the elements. The intensity of the shorter wavelength line increases with the atomic number. We note, however, that the shorter wavelength $J = 0$-1 line intensity has dominated for Yb, Ta, and W [1]. According to the calculated oscillator strengths for both of the $J = 0$-1 lines shown in Table I, the oscillator strength increases with Z for the shorter wavelength line, and vice versa for the longer wavelength line. This tendency is in agreement with the present and the previous experiments. The calculated oscillator strengths for the two $J = 0$-1 lines become approximately equal for Gd, but the radiative decay time from the lower lasing level of the shorter line to the ground state is twice that from the longer line to the ground state as shown in Table I. The upper level of the $J = 0$-1 lines is pumped predominantly by the monopole electron collisional excitation [19]. A simplified rate equation analysis including the upper and the lower lasing levels and the ground state for Gd gives the ratio of the gain coefficients (that of the shorter wavelength line to that of the longer one) as ~0.9. The result agrees qualitatively with the experimental result. The calculation used the radiative constants given in Table I.

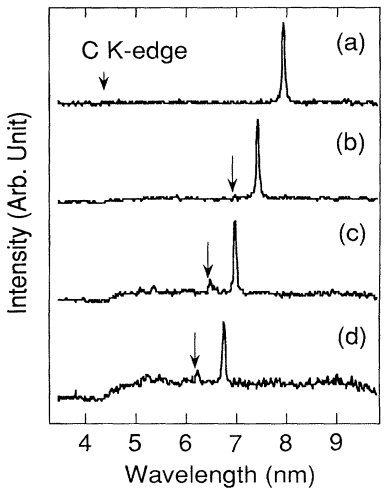

FIG. 1. Typical spectra of (a) Nd, (b) Sm, (c) Gd, and (d) Tb recorded with the flat field spectrometer and the x-ray streak camera. The shorter wavelength $J = 0$-1 lines are indicated by the arrows. The relative peak intensities of the longer wavelength $J = 0$-1 lines are 12.8, 4.3, 2.1, and 1.0 for Nd, Sm, Gd, and Tb, respectively. The gain lengths are 2.5 cm.

The beam divergence of the Nd $J = 0$-1 longer wavelength lasing line was measured by placing angular fiducial wires at the entrance of the spectrometer. The angle is ~4 mrad (FWHM) which corresponded to the coherence length of ~1 μm at the end of the lasing medium.

Figure 2 shows the dependence of the relative x-ray laser intensities on the gain length for the Ni-like isoelectronic sequences. The gain coefficients derived with the Linford formula [20] of the longer wavelength $J = 0$-1 line of Nd (7.97 nm), Sm (7.32 nm), Gd (6.92 nm), and Tb (6.67 nm) are 3.1 ± 0.1, 2.6 ± 0.1, 2.8 ± 0.2, and 4.0 ± 0.8 cm^{-1}, respectively. For Nd, the gain-length product corresponds to 7.8 by pumping with double pulses of 250 J energy on a 2.5-cm-length target. The gain coefficient of the shorter wavelength $J = 0$-1 line of Gd (6.39 nm) is ~2 cm^{-1} derived from the intensity ratio of its two $J = 0$-1 lines shown in Fig. 2. A similar intensity ratio is found for Tb.

Figures 3(a), 3(b), and 3(c) show the temporal profiles of the lasing lines for Tb and Nd pumped by double pulses and for Nd pumped by triple pulses, respectively. The target lengths were 2.5, 1.7, and 2.0 cm for Figs. 3(a), 3(b), and 3(c), respectively. Also shown in Fig. 3(b) by curve C is the time history of the incoherent x-ray emission band whose wavelength is between 4 and 6 nm (N and O shell

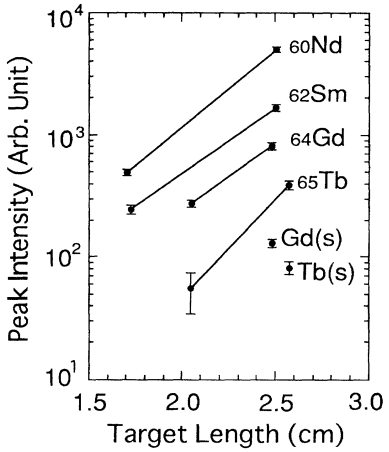

FIG. 2. The relative peak intensities of the longer wavelength $J = 0\text{-}1$ lines as a function of the gain length. The symbols Nd, Sm, Gd, and Tb represent, respectively, the longer wavelength lines of Ni-like ions of these species. The symbols Gd(s) and Tb(s) represent the peak intensities of the shorter wavelength line of Gd and Tb, respectively.

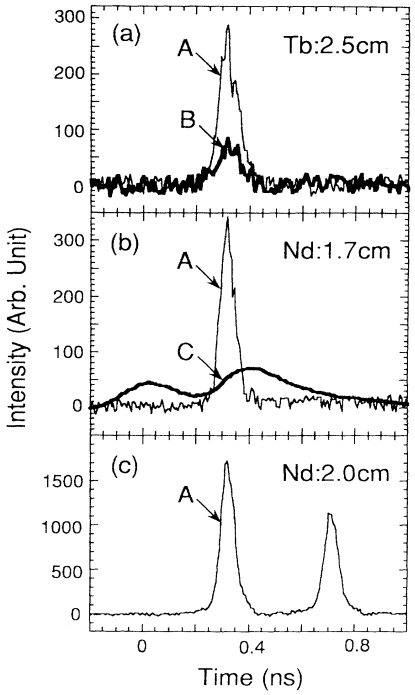

FIG. 3. Temporal profiles of the $J = 0\text{-}1$ lines of Tb in (a) and Nd in (b) and (c). The notations A, B, and C denote, respectively, the temporal profile of the longer wavelength $J = 0\text{-}1$ line, the shorter wavelength $J = 0\text{-}1$ line, and the background continuum x ray. Each pumping pulse contains ~130 J, and each pulse-to-pulse separation is 400 ps.

emissions). The duration is ~160 ps, which is longer than the 100-ps pumping width due to the 60 ps photon traversal time over the plasma length. For Tb the temporal profiles of the two $J = 0\text{-}1$ lasing lines are shown by curves A and B in Fig. 3(a). We find that lasing does not take place at the first pumping pulse (time ~0 s in Fig. 3), similar to the observed behavior for Ne-like Ge [13]. In Fig. 3(b), the Nd x-ray laser has a pulse width of ~70 ps (FWHM) and its intensity becomes maximum at 80 ps before the peak of the second incoherent x-ray pulse. Although the exact timing of the x-ray laser pulse is unknown relative to the pumping laser pulse, our simulation shows that the peak of the incoherent x-ray pulse is delayed by ~80 ps from the peak of the pumping pulse. Thus the peak of the x-ray laser pulse coincides approximately with the pumping pulse. The result also suggests that a similar gain may be obtained at the same irradiation intensity but with a shorter duration and thus a smaller laser energy.

The time dependence of the gain has been calculated for the Nd laser (1.7 cm length) from the measured x-ray laser wave form shown in Fig. 3(b) and the gain length dependence shown in Fig. 2 on the basis of a calculation model of amplified spontaneous emission [21] including finite gain history and photon transport. The calculation shows that the gain becomes maximum at the peak of the x-ray laser pulse with a peak gain coefficient of 3.5 cm^{-1}. Both the rise time and the FWHM of the gain are approximately ~130 ps. The measured soft x-ray laser pulse duration decreases to ~60 ps for a 2.5-cm-length target as shown in Fig. 2(c), in agreement with the model calculation. The model calculation also predicts that a twice higher x-ray laser intensity will be obtained if traveling wave pumping is used for a 2.5-cm-long Nd laser. As shown in Fig. 3(c), triple pulse pumping generates a double-pulse x-ray laser. This shows a possibility for generating a significantly higher brightness x-ray laser with better coherence by double pass amplification using a soft x-ray mirror (of ~10% reflectivity at this wavelength) at one end of the target.

In summary, we have described multiple infrared pulse pumping of Ni-like lanthanide elements with a curved target. The required pumping energy is ~250 J, which is an order of magnitude less than the value in the previous Ni-like lasers, giving significant improvement in the pumping efficiency for the $J = 0\text{-}1$ $(\frac{3}{2}, \frac{3}{2}) \rightarrow (\frac{5}{2}, \frac{3}{2})$ transition with the wavelength range between 6 and 8 nm. The optimum electron density is a few times 10^{20} cm^{-3} for these x-ray lasers. The 1 μm wavelength laser heats the plasma efficiently over the appropriate absorption scale length preformed by a prepulse. The desired shape of the transverse and axial plasma controlled by the double-pulse pumping and the curved target techniques for maximizing gain region and minimizing refraction loss, respectively, provides efficient Ni-like lasers. The output power of the Nd x-ray laser is estimated to be on the order of ~10 kW (energy ~1 μJ), derived from comparison between the intensities of the Ge laser and the

Nd laser taking into account the filter transmission, the grating efficiency, and the sensitivity of the detector.

The energy gap of the Ni-like ground state and the upper lasing level is twice as large as the electron temperature which maximizes Ni-like abundance. Actually, 2 or 3 times higher electron temperature increases the excitation rate significantly [19]. Early peaking of the short x-ray laser pulse obtained in our experiment may suggest that a highly nonequilibrium lasing medium which is transient to the next ionization stage has been produced because the monopole excitation rate is 1 order of magnitude larger than the ionization rate. With this concept, a long pulse laser creates Ni-like ions and a successive short intense laser pulse (a few tenths of ps) creates the desired electrons for monopole excitation. The latter pulse should be short enough to minimize further ionization. For the shorter wavelength lasers towards the water window spectral region [22], such a high intensity short pulse pumping scheme with a prepulse technique will make significant reduction of the pumping energy.

The authors are indebted to the glass laser operation group and the target fabrication group for the technical support for this work. This work was partly supported by the Grant-in-Aid for Scientific Researches of the Ministry of Education, Science and Culture (No. 06680447).

[1] B. J. MacGowan *et al.*, Phys. Fluids B **4**, 2326 (1992), and references therein.
[2] A. Carillon *et al.*, Phys. Rev. Lett. **68**, 2917 (1992).
[3] L. B. Da Silva *et al.*, Opt. Lett. **18**, 1174 (1993).
[4] M. D. Rosen *et al.*, Phys. Fluids **31**, 666 (1988).
[5] H. Takabe and T. Nishikawa, J. Quant. Spectrosc. Radiat. Transfer **51**, 379 (1994).
[6] S. Maxon *et al.*, J. Appl. Phys. **57**, 971 (1985).
[7] B. J. MacGowan *et al.*, Phys. Rev. Lett. **59**, 2157 (1987).
[8] B. J. MacGowan *et al.*, J. Opt. Soc. Am. B **5**, 1858 (1988).
[9] B. J. MacGowan *et al.*, Phys. Rev. Lett. **65**, 420 (1990).
[10] J. G. Lunney, Appl. Phys. Lett. **48**, 891 (1986).
[11] R. Kodama *et al.*, Phys. Rev. Lett. **73**, 3215 (1994).
[12] S. Basu *et al.*, Appl. Phys. B **57**, 303 (1993).
[13] H. Daido *et al.*, Opt. Lett. **20**, 61 (1995).
[14] T. Kita *et al.*, Appl. Opt. **22**, 512 (1983).
[15] K. Murai *et al.*, J. Opt. Soc. Am. B **11**, 2287 (1994).
[16] K. G. Dyall *et al.*, Comput. Phys. Commun. **55**, 425 (1988).
[17] J. Scofield and B. J. MacGowan, Phys. Scr. **46**, 361 (1992).
[18] Lasing was not observed for Eu and Sm when fluorides (EuF_2 and SmF_3) were used as the lasing material due probably to the dilution effect.
[19] P. L. Hagelstein, Phys. Rev. A **34**, 874 (1986).
[20] G. J. Linford *et al.*, Appl. Opt. **13**, 379 (1974).
[21] L. B. Da Silva *et al.*, Opt. Lett. **19**, 1532 (1994).
[22] S. Maxon *et al.*, Phys. Rev. Lett. **70**, 2285 (1993).